

The tribological performance of coated and non-coated materials in high temperature environments

Chinchilla Adell, R.F.¹; Burkinshaw, M.²; Lindsay, M.²; Proprentner, D.¹ and Shollock, B.¹

¹WMG Warwick Manufacturing Group, University of Warwick, Coventry, CV4 7AL, UK.

²Cummins Turbo Technologies (CTT), Huddersfield, HD1 6RA, UK.

© [Raul Chinchilla Adell, 2018]. The definitive version of this article is published in the 13th International Conference on Turbochargers and Turbocharging, **Institution of Mechanical Engineers**, 2018

Abstract:

Variable geometry (VG) and wastegate mechanisms are commonplace within modern turbochargers and contain critical components without which the correct and efficient operation of a turbomachine would be affected. Such mechanisms rely upon components repeatedly and accurately moving against one another, even when subjected to extreme conditions such as high temperatures, a range of exhaust gas chemistries and in dry conditions. Therefore, the materials used within typical VG and wastegate mechanisms need to possess corrosion and oxidation resistance as well as the required mechanical properties at high temperatures. Conventional materials with such characteristics, however, do not necessarily possess adequate friction and wear behaviour. Hence, there is a desire to investigate the benefit of using alternative materials, such as nickel and cobalt based superalloys, but their use in these applications is limited by their cost. A coated base alloy provides a wider pool of possible solutions and the ability to achieve a more cost-effective solution. By taking into consideration the environments to which VG and wastegate components are subjected, a time efficient selection process was developed that takes engineering and purchasing requirements into consideration. The material and coating samples were subjected to different conditions which are typically experienced during turbocharger operation in order to understand their corrosion and oxidation behaviour, with the worst performing concepts removed from the testing matrix. Subsequently, tribology testing was conducted using the remaining concepts, at temperatures typical of turbocharger operation, and the friction and wear results were compared. All concepts were characterised by using confocal microscopy, high resolution microscopy, chemical analysis and nanoindentation in order to understand their performance. The results were compiled in a matrix in order to determine, from an engineering and purchasing perspective, which concepts were most suitable for application within high temperature, turbocharger-based, tribological environments.

1. Introduction

Turbochargers are devices used fundamentally to reduce emissions, increase power and minimise fuel consumption of the internal combustion engine. The components in the turbine end of the turbocharger experience high temperatures and highly corrosive environments, which are dependent on the fuel source used; petrol, diesel or natural gas. The VG and wastegate mechanisms located within the turbocharger

turbine stage must provide reliable operation and predictable friction and wear performance throughout the lifetime of the turbocharger, up to 1 million miles.

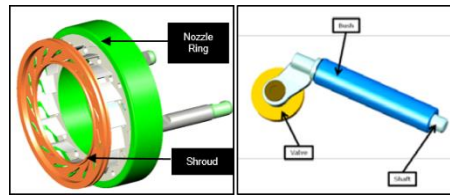


Figure 1. Typical CTT VG mechanism (left) and wastegate (right) (1).

To meet these requirements, components are typically produced from stainless steels. However, when subjected to extreme environments, the wear and friction characteristics provided by such materials are not sufficient for the application, resulting in durability and reliability issues.

Co-based alloys have higher strength, and meet the corrosion and tribological performance (2, 3) over the operation temperature range of a turbocharger, making them an attractive alternative from an engineering perspective. However, the cost and global acquisition of such materials is prohibitive from a purchasing perspective (4, 5). Therefore, cost effective and globally available alternatives, which provide appropriate tribological and environmental performance, need to be identified.

Coatings are a technology that creates a highly specialised cost-effective composite that helps provide superior corrosion, wear and/or friction performance to cheaper, and lower capability alloys (6). From a tribological perspective, coatings, such as TiN, started to be used by the tool industry to improve tool life (7). From a corrosion/oxidation perspective, pack diffusion coatings, such as aluminiumizing, are good candidates due to their price relative to the plasma vapour deposition (PVD) options (such as TiN), and the formation of high temperature stable oxides, such as Al_2O_3 (8).

The aim of this article is to present a suitable material selection process for tribological applications and the characterization of the tribological performance of the selected materials by representing the contact in a tribometer laboratory-based test. An austenitic stainless steel, two Co-based alloys, a Cr-based diffusion treatment, an Al-based diffusion treatment and an AlTiN PVD coating were tested at three different temperatures, 250°C, 650°C and 760°C, in order to understand their tribological performance over the wide operation range of the turbocharger. High resolution surface topographical analysis and scanning electron microscopy (SEM) were used to understand the wear volume and the wear mechanisms experienced by the materials under evaluation. Energy-Dispersive X-ray spectroscopy (EDX) was used in order to understand the chemical changes experienced in the contact.

2. Experimental

2.1. Material Selection Process

One of the advantages of coatings as engineering solutions is the wide range of available alternatives, but it can also be detrimental since it is challenging to determine the most effective and appropriate solution within a given time period. As a result, it is commonplace to evaluate concepts and discard using a suitable selection process. Matthews, Holmberg and Frankling (9) have previously introduced a 9-stage process, which takes into consideration both engineering and purchasing requirements for a given application. The engineering and purchasing requirements

which were under consideration for this project are given in Table 1. These requirements were applied during the concept filtering process shown in Figure 2.

Table 1. Elements taken into consideration during the selection process.

Engineering requirements	Purchasing requirements
Adhesion	Intellectual proprietary
Corrosion resistance	Environmental compliance
Thermal shock	Cost
Thermal capability	Dual source/global availability
Surface treatment uniformity	-
Surface finish requirements	-
Component dimensional changes	-
Tribological characteristics	-

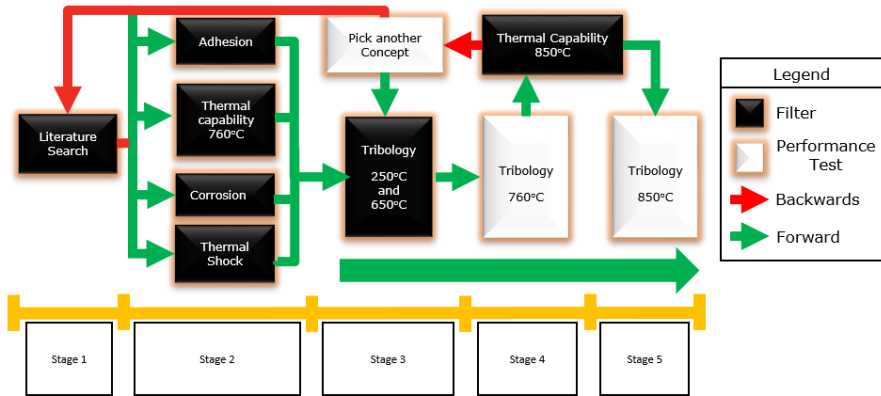


Figure 2. Filtering process diagram

All concepts evaluated in this article were ranked in terms of their performance, with different importance weightings given to the various sections of Table 1. A cause and effect (C&E) matrix was used to score the concepts based upon the different engineering and purchasing requirements and the performance demonstrated by the concepts in the tests described in this article. Following the filters; at stage 2, two of the concepts were discarded prior to the tribology test; and at stage 3, two more concepts were discarded. During stage 2 of the selection process, material characterisation is required for the understanding of the behaviour of the material from a mechanical, physical and chemical perspective.

2.2. Materials

Several coatings were evaluated and compared against three base line materials; these are listed in Table 2. Note that all coatings were applied to the austenitic stainless steel.

Table 2. Materials at stage 2 of the selection process

Material	Coating Thickness
Austenitic Stainless Steel	-
Boronizing	23µm
Chromizing	33µm
Aluminiumizing	52µm
Nitriding	109µm
AlTiN	3µm
Cobalt alloy 1	-

2.3. Methods

2.3.1. Adhesion

VDI 3198 standard testing (10) was used to understand the adhesion performance of the coating to the substrate. The test uses a Rockwell C tester and a diamond conical indenter, to make an indent using 150kg force. After the test was carried out, samples were observed under an optical microscope and the failure mechanism of the coatings was ranked according to the standard. Depending on how they failed, a score between H1 to H6 was given to each coated concept. H1 to H4 was regarded as a pass, while H5 to H6 was a failure.

2.3.2. Oxidation/Thermal stability

Oxidation/thermal stability testing was performed in a muffle furnace at 760°C for 250h with test samples of size 35.6mm x 25.4mm x 10mm. Oxidation behaviour was measured by reviewing the thickness of the oxide layer, the depth of the internal oxidation and oxide layer spallation, together with microstructural and chemical changes.

2.3.3. Corrosion

For the corrosion test, a solution composed of 2L of water, 100g of NaCl and sufficient H₂SO₄ to achieve a pH value of 5 was used. A volume of 45ml was applied to the samples presented in Table 2. The samples, with size 35.6mm x 25.4mm x 10mm, were subsequently placed in a sealed container for 24h. All samples were cleaned and new solution was applied in 24h cycles up to 250h. The corrosion performance was determined by reviewing the surface/coating damage, surface compounds formed and the ability of the coating to prevent damage to the underlying substrate.

2.3.4. Thermal Shock

A K-type thermocouple was welded on a sample of size 2mm x 2mm x 2mm which was placed in a 760°C pre-heated muffle furnace. When the sample reached 760°C, it was removed from the muffle furnace and left to air cool. This procedure was carried out 8 times per sample. Samples were inspected by optical microscopy for signs of cracking.

2.3.5. Surface Topography

Surface Topography was obtained by using an Alicona™ InfiniteFocus® microscope. Measurements were carried out on three plates and pins at a magnification, lateral and vertical resolution of x20, 1.25µm, and 1.00µm, respectively. 3D surface topography measurements were performed using a 4mm x 4mm square and a cut-off wavelength of 800µm. Measurements comply with ISO25178/12781-1. Surface topography characteristics were defined using S_a, S_z and S_q parameters.

2.3.6. Nanoindentation

Mechanical properties of all samples were acquired from cross-sections of the samples using a nanoindenter with a Berkovic style diamond indenter. A depth control experiment was used in which the indenter reached a maximum depth of 250nm. The loading and unloading rates were 0.5mN/s and 0.5mN/s respectively, with a dwell time of 5s and an indent separation of 7µm. For coating materials, indents along the coating thickness were made. For bulk materials, 100 indents were made. Finally, AlTiN mechanical properties were obtained from literature (11), as currently non-reliable values were obtained.

2.3.7. Tribology Testing

The evaluation of the tribological performance of the sample was conducted using an Rtec multifunction pin-on-reciprocating plate tribometer. For this article, a variable geometry mechanism was modelled, with the pin representing the shroud and the plate representing the nozzle. The material pairs that underwent the test are shown in Table 3 and the contact conditions, which were designed to replicate the conditions experienced by the components in operation, are shown in Table 4.

Table 3. Material pairs under tribological evaluation.

Pin/Plate
(Austenitic Stainless steel)/(Austenitic Stainless steel)
(Chromizing)/(Chromizing)
(Aluminiumizing)/(Aluminiumizing)
(AlTiN)/(AlTiN)
(Cobalt alloy1)/(Cobalt alloy2)
(Cobalt alloy2)/(Cobalt alloy1)

The geometry of the pin and the maximum contact stress during the test were calculated by doing a Hertzian analysis using Equations 1-3 (12), when a load of 4N is applied on the test:

$$\frac{1}{E^*} = \frac{1 - \nu_1^2}{E_1} + \frac{1 - \nu_2^2}{E_2}$$

Equation 1(1)

$$a_c = \left[\frac{3PR}{4E_c} \right]^{1/3}$$

Equation 2(1)

$$p_o = \frac{3}{2} \frac{P}{\pi a_c^2}$$

Equation 3(1)

Table 4. Tribological test parameters.

Maximum Contact Pressure	90MPa
Stroke Length	5mm
Frequency	6Hz
Operating Temperatures	250°C, 650°C and 760°C
Atmosphere	Air
Test Duration	2h

2.3.8. Evaluation of worn samples

High magnification images of the surface were obtained using ZEISS Sigma, FEI Scios, FEI Versa and Jeol 7800 field emission SEMs. Chemistry information of the surface was obtained by using EDX. Wear volume was obtained using an Alicona™ InfiniteFocus® with 5x magnification, with the raw data analysed using bespoke Matlab code in order to provide the most reliable results.

3. Results

3.1. Selection Process Pre-Tribology testing

3.1.1. Adhesion

All surface treatment concepts possessed a score of H2, except nitriding which was ranked H3.

3.1.2. Thermal capability/Oxidation

From a visual inspection the austenitic stainless steel, chromizing, and AlTiN showed the formation of a resilient oxide layer, while boronizing, aluminiumizing, and nitriding showed partial oxide layer delamination. EDX analysis of the surface was carried out to confirm the observation.

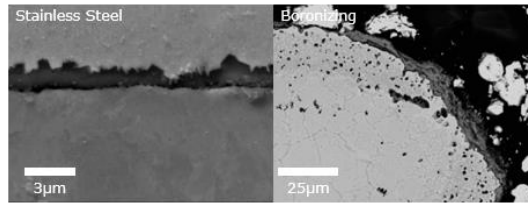


Figure 3. SEM image of best (left) and worst (right) performing materials on the thermal stability test.

Figure 3 shows the cross-sections of the best performing material, austenitic stainless steel, and the worst performing material, boronizing. The stainless steel, chromizing, and aluminiumizing samples show a thin oxide layer. Nitriding possessed a smooth, thick oxide layer, but it seems that oxidation products were also formed within the coating. AlTiN showed a dual component oxide layer composed of Al-base oxide on top of Ti-base oxides, but the substrate shows internal oxidation just below the coating, which can grow through the coating reaching the surface. Boronizing showed a poor stability oxide layer with the addition of internal oxidation and an increase in porosity. For all diffusion treatments change in the initial microstructure and the elemental distribution were observed.

3.1.3. Corrosion

Figure 4 shows images of the samples before and after the application of the fluorescence compound for inspection. The Cr-oxide formers, austenitic stainless steel and chromizing, slightly suffered from pitting, while aluminiumizing and AlTiN formed Al and Fe base oxide compounds on the surface. Nitriding shows the formation of a thick oxide layer. Boronizing experienced both behaviours, in terms of high oxidation and pitting.

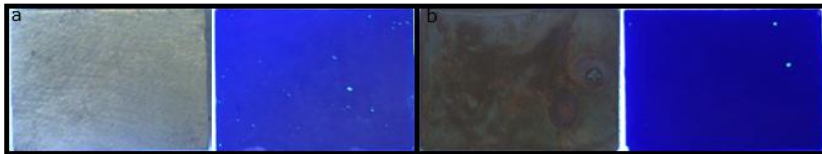


Figure 4. Test coupons after corrosion test of (a) stainless steel and (b) boronizing showing surface pitting and, pitting and heavy oxidation, respectively.

3.1.4. Thermal Shock

All concepts possessed acceptable thermal behaviour since no cracks were evident on any concepts under evaluation.

3.2. Surface Topography

At this point the nitriding and boronizing concepts possessed the lowest weightings and were removed from the selection process, which will be further discussed in Section 4.1.

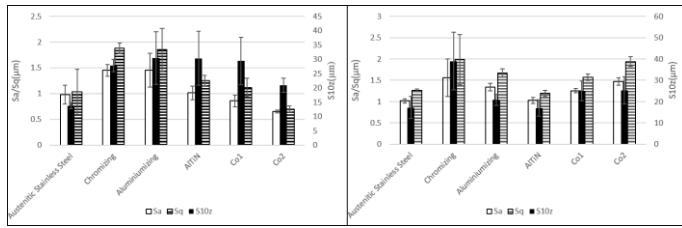


Figure 5. Topography measurements of coated and uncoated materials pin (left) and plate (right).

Figure 5 presents surface properties of the pin and plates. The stainless steel and AlTiN samples showed similar values of S_a , S_z ; while S_q shows an increase in value. Although sample machining was the same for all bulk materials, the Co-based alloys showed small deviations from the stainless steel; lower values for Cobalt2 pin and higher values for Cobalt1 and Cobalt2 plate. Finally, chromizing and aluminumizing exhibited an increase of all surface topography values for both pin and plates.

3.3. Nanoindentation

Figure 6 shows the data gathered using nanoindentation in terms of Hardness (H) and Reduced Elastic Modulus (Reduced E). For the Co-alloys, two types of material behaviour were identified; these relate to (a) the matrix and (b) the combined behaviour of the hard particle and the matrix.

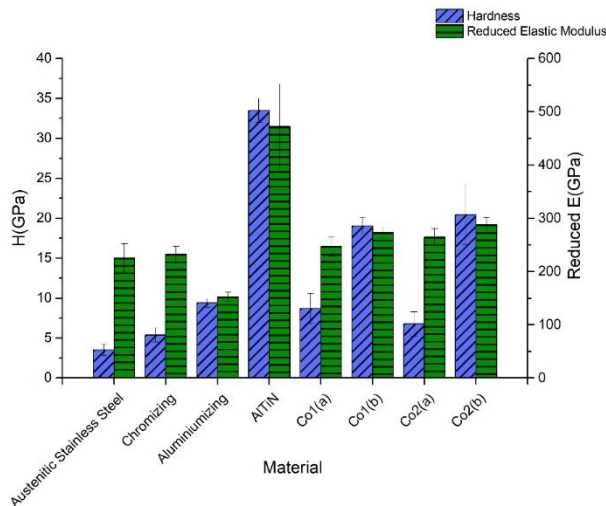


Figure 6. Mechanical properties of coated and uncoated materials. For Co1 and Co2, (a) and (b) mean matrix and combination of matrix and hard particles respectively.

3.4. Friction

Figure 7 presents the coefficient of friction (CoF) of the material combinations at 250°C, 650°C and 760°C. A reduction in friction was experienced by materials as the temperature increased, except for chromizing where the CoF remained similar at 650°C and 760°C. In addition, the CoF of aluminiumizing remained the same over both tested temperatures, and that of combination Co2/Co1 increased at 650°C.

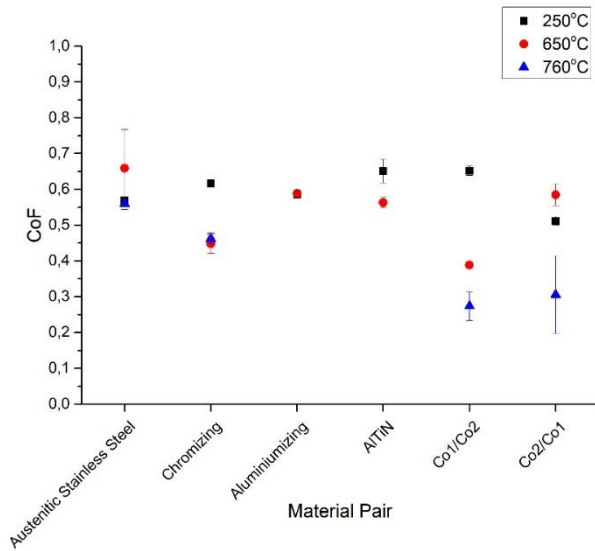


Figure 7. Friction performance of concepts at the tested temperatures.

3.5. Volumetric wear

Figure 8 shows the wear volume of all the material plates at 250°C, 650°C and 760°C. Pin data is not reported due to repeatability issues associated with pin topography and geometry. The aluminiumizing plate had the poorest performance at all the tested temperatures, followed by the austenitic stainless steel. The plates manufactured from the Co-based alloys had the best performance closely followed by the AlTiN plate at the temperatures tested.

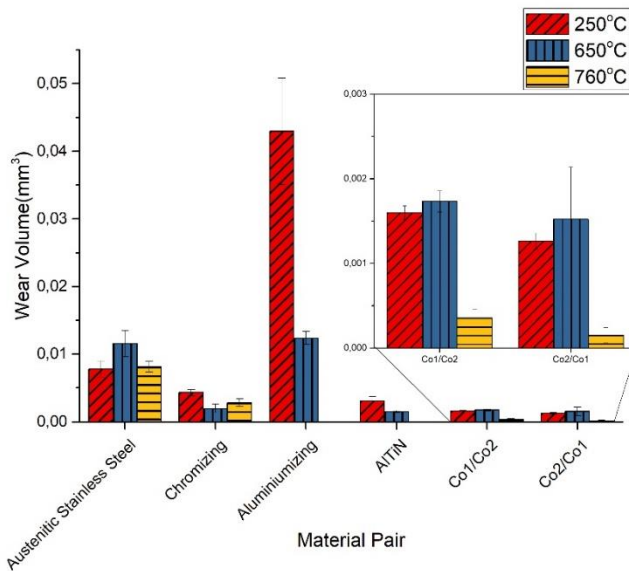


Figure 8. Measured wear volume observed on the plates of each sample at the tested temperatures.

3.6. Morphology and chemistry of wear scars

3.6.1. 250°C

Figure 9 shows the wear scars generated on the pin and plate of each sample at 250°C using SEM. The stainless steel pair showed extremely coarse wear tracks and smoother areas where cracks were found growing perpendicular to the direction of motion. Chromizing exhibited a similar but less pronounced behaviour compared to the stainless steel. Aluminiumizing showed extremely rough areas at the sides of the wear scar, as well as highly smooth areas in the middle of the wear scar. AlTiN showed a similar behaviour to chromizing. For the Co-based alloy pairs, the surfaces were highly polished.

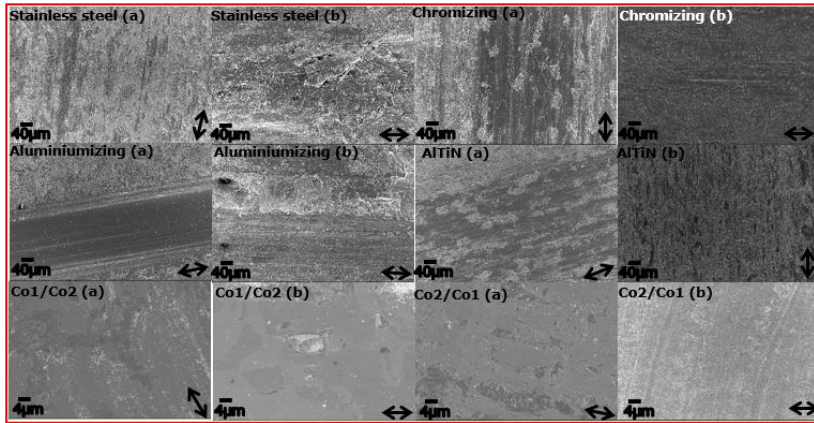


Figure 9. InLens SEM images of the wear scars of the pins (a) and plates (b) subjected to tribology testing at 250°C. Arrows indicate the direction of sliding.

Figure 10 presents the EDX maps of concepts tested at 250°C. The main elements detected in the wear scars are shown on the right-hand side of the figure. Oxygen was prevalent for all material combinations. In addition, aluminiumizing and AlTiN possessed an apparent decrease in Al content in the wear scar.

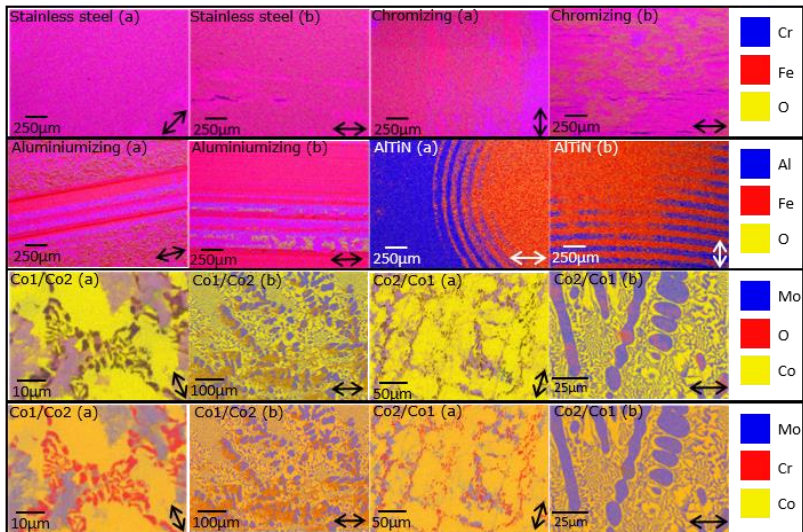


Figure 10. Chemical maps of the wear scars of the pins (a) and plates (b) subjected to tribology testing at 250°C. Arrows indicate the sliding direction

3.6.2. 650°C

Figure 11 shows the wear scars generated on the pin and the plate at 650°C. The stainless steel, chromizing, aluminiumizing and AlTiN concepts possessed coarse wear tracks alongside smoother areas. Co1/Co2 pair exhibited a smooth wear scar, while the wear scars of Co2/Co1 pair were slightly rougher.

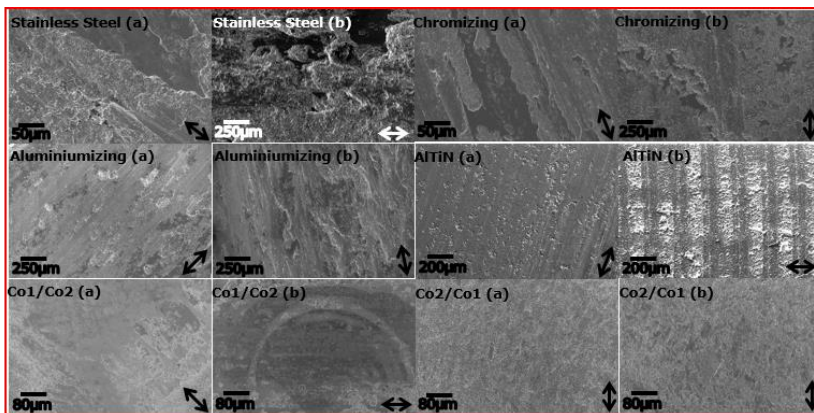


Figure 11. InLens SEM images of the wear scars of the pins (a) and plates (b) subjected to tribology testing at 250°C. Arrows indicate the direction of sliding.

Figure 12 presents the EDX maps of the samples at 650°C. For all cases, the EDX showed a higher relative oxygen concentration than at 250°C. AlTiN behaved similarly at both temperatures with the appearance of Al deficient areas. On the pin of the Co1/Co2 pair and the plate of the Co2/Co1 pair higher relative concentrations of Mo were found on the surface.

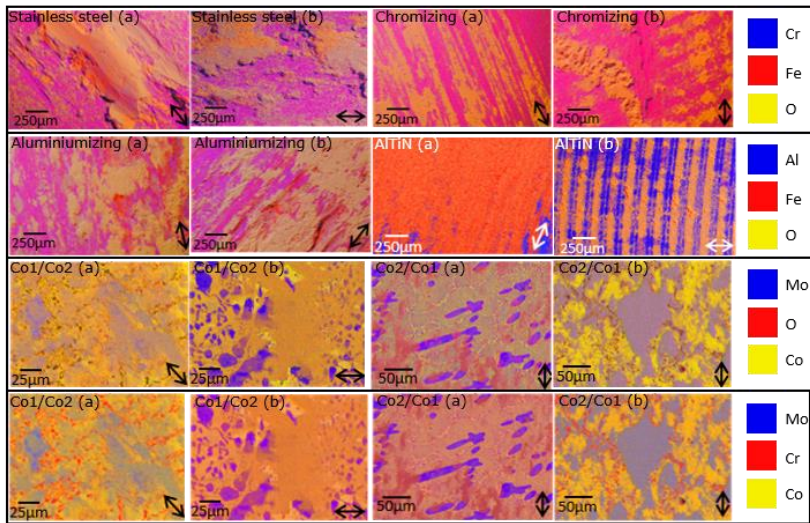


Figure 12. Chemical images of the wear scars of the pins (a) and the plates (b) subjected tribology testing at 650°C. Arrows indicate the direction of sliding.

3.6.3. 760°C

Figure 13 shows the wear scars generated on the pin and plate at 760°C. Stainless steel and chromizing pairs possessed coarse wear scars, alongside smooth dark areas. In contrast, Co1/Co2 pair and Co2/Co1 pin exhibited smooth the wear scars. Co2/Co1 plate possessed a smooth scar on the outside, while the middle appeared to suffer from heavy abrasion.

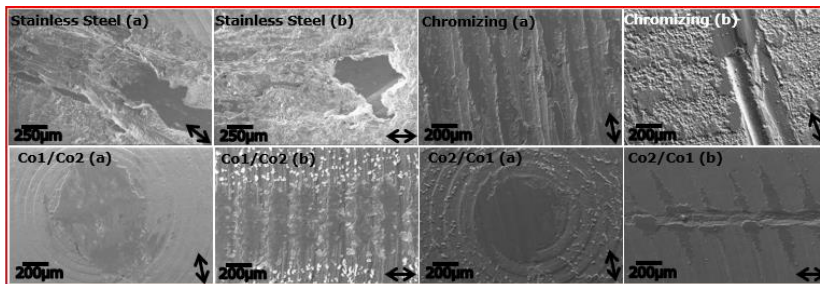


Figure 13. InLens SEM images of the wear scars of the pins (a) and the plates (b) subjected to tribology testing at 760°C. Arrows indicate the direction of sliding.

Figure 14 presents the EDX maps of the samples tested at 760°C. Similar to the 650°C temperature, at 760°C heavily oxidised areas can be observed. For the stainless steel and chromizing pair, a higher relative concentration of Cr was witnessed on the surface. For the Co1/Co2 and Co2/Co1 pairs, higher Co, Cr and O relative concentrations on the surface.

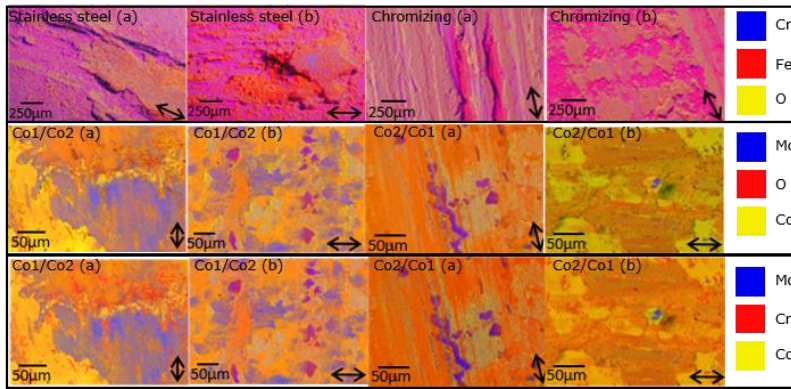


Figure 14. Chemical images of the wear scars of the pins (a) and the plates subjected to tribology testing at 760°C. Arrows indicate the direction of sliding.

4. Discussion

4.1. Selection process

A successful selection process has been developed to identify suitable material pairs for high temperature tribological applications for high temperature turbocharger applications. A similar approach as the selection process proposed by Matthews, Holmberg and Frankling was taken, in which engineering requirements were developed to match the application requirements and the purchasing requirements from a non-functional, economic and procurement perspective. But in this case, these requirements for the application are listed and key requirements were used as filters to improve time-efficiency. Requirements were compared and contrasted using a C&E matrix to define the treatments that will follow to the consecutive testing stages.

Nitriding and boronizing were removed following the first stage of selection due to poor engineering performance, even though the concepts were good from a purchasing perspective. Boronizing performed worst from a corrosion and thermal stability perspective, and, due to the nature of the treatment, it caused dimensional changes of the components. While nitriding did not cause dimensional changes, it performed worse than other samples from a corrosion, thermal stability and adhesive perspective.

At the second stage, aluminiumizing and AlTiN were overall outperformed by chromizing, because the tribological properties in conjunction with the other engineering and purchasing requirements ranked chromizing higher on the C&E matrix.

The following sub-sections discuss the reasons behind the elimination decisions at the different stages in more detail.

4.1.1. Adhesion

All concepts scored equally with the exception of nitriding. The probable reason of nitriding being outperformed by the other coating concepts was the brittleness and the high case hardening thickness. This is important as coating failure due to high applied load can cause a catastrophic tribological failure.

4.1.2. Thermal capability/Oxidation

The baseline material, austenitic stainless steel, performed better than the coating concepts because of the microstructural stability of the oxide, which was composed of an outer Cr-base oxide followed by a Si-based. This Si-based oxide provides additional oxidation resistance at high temperatures. Chromizing and aluminiumizing had a similar thermal performance, but their poorer performance relative to the austenitic stainless steel was due to these materials undergoing microstructural changes. These changes were caused by the continuous diffusion of the main element used for the coating formation, caused by the chemical potential difference between the transformed layer and the substrate. In addition, due to the density of the coating or the existence of uncoated areas, AlTiN coating showed internal oxidation of the substrate material, which could grow both inwards and outwards from the substrate.

Finally, the worst performing treatments were boronizing and nitriding, which underwent microstructural changes, internal oxidation, porosity growth and possessed an unstable oxide layer. These changes were caused by a range of factors, including the chemical potential between coating and substrate, an oxygen permeable external oxide layer, the formation of Fe-based oxides (caused by reduction of chromium available due to the formation of (FeCr)B and CrN compounds/precipitates respectively (13-15)), and the formation of a thick and high density defect oxide layer.

4.1.3. Corrosion

The superior corrosion performance of aluminiumizing can be attributed to the formation of Al-based oxides on the surface of the material (8). Slight pitting was observed on the surface of the austenitic stainless steel and chromizing due to the re-dissolving of the Cr-based products comprising the passivating layer on the surface. This leads to pit nucleation sites as the corrosion process reactivates (8). Varying degrees of Fe-based corrosion products were observed on nitriding and AlTiN. For nitriding, the coating served as a sacrificial corrosion layer, keeping the substrate material protected. Oxides could be observed forming in the coating; this was probably due to intergranular corrosion (13, 14). For AlTiN, the substrate was also affected by corrosion due to poor coating density or coverage. Finally, for boronizing, the formation of Fe-based oxides was due to the use of Cr in the formation of (FeCr) B_x (x=1, 2) layers. Pits could have been caused by localized corrosion, which can be attributed to the inherent formation of microcracks and porosity of this coating (15).

4.2. Tribological performance

Reviewing the data, shows that the materials with best wear properties in this study are the cobalt alloys over the whole temperature range; which is well documented in literature (2-5). The performance of AlTiN was like both Co-superalloy pairs. However, AlTiN did appear to slowly be removed during tribology testing as shown by Figures 10 and 12, which questions its long term durability performance. Aluminiumizing performed worse than the base austenitic stainless steel.

Overall, from a wear perspective, a decrease in the wear volume was observed due to the formation of compacted layers or highly deformed oxide layers in most of the samples at the different tested temperatures. The stability of these compacted layers was related to their mechanical properties. This in turn relates to the load capacity of the layered system and the oxidation behaviour, which refers to the mechanical properties and the chemistry of oxides, and the oxidation rate of the surface material.

By reviewing the wear mechanisms acting on the system, the wear volume and their friction behaviour, the different materials can be classified at the different test stages as shown in Table 5. The best performing candidate was represented by a 1. The worst performing candidate was represented by a 6 at 250°C and 650°C, and by a 4 at 760°C.

Table 5. Ranking of the different concepts from a wear and friction perspective at the different test temperatures. Numbers indicate the best (1) performing material pair and the worst (6 / 4) for each temperature.

	Wear			Friction		
	250°C	650°C	760°C	250°C	650°C	760°C
Austenitic Stainless Steel	5	5	4	3	6	4
Chromizing	4	4	3	4	2	3
Aluminiumizing	6	6	-	2	4	-
AlTiN	3	3	-	6	3	-
Co1/Co2	2	1	1	5	1	1
Co2/Co1	1	2	2	1	5	2

By considering all engineering requirements, the overall performance of the concepts can be classified from best to worst as follows:

1. Co1/Co2
2. Co2/Co1
3. Chromizing
4. AlTiN
5. Austenitic stainless steel
6. Aluminiumizing

As mentioned earlier, cobalt based alloys are prohibited from a purchasing perspective. Some coatings, such as AlTiN, can offer similar wear behaviour to such alloys. Alternatives, such as chromizing, are preferable from a purchasing perspective. In addition, chromizing did not fail during testing, provided better friction behaviour and a high overall engineering and purchasing ranking. It must be noted that it is a necessity of bulk materials to be designed and selected appropriately for a given application; a similar approach needs to be taken for coatings.

5. Conclusion

A wide range of materials and coatings were evaluated in simulated laboratory environments to evaluate their thermal capabilities, mechanical properties and corrosion performance. The best performing concepts were subjected to tribology testing in the conditions simulating those experienced between a turbocharger nozzle ring and shroud, or for the wastegate interface.

A selection process for high temperature tribological applications for turbomachinery was presented. It combined a testing flow, filters to understand how the system can be compromised and a C&E matrix which used engineering and purchasing requirements to indicate the most favourable direction depending on importance for the application.

The performance of the concepts was ranked based on the results obtained from the various tests and purchasing considerations, with the best candidate(s) being selected.

From an engineering perspective, including the tribological aspect, the Co-base alloys outperformed the coating concepts. Coating materials offer benefits from a purchasing perspective; such as chromizing, and can favourably compete against the Co-base alloys from a tribological perspective; as shown by AlTiN. Overall, chromizing on top of the other concepts as it had similar or better performance from a purchasing and engineering, including friction, perspective. However, if a minimum wear resistance was required, that condition could change the end result to more wear resistant coatings such as AlTiN.

6. Acknowledgements

This material is based upon work supported by EPSRC Engineering Doctoral Center in High Value, Low Environmental Impact Manufacturing. Further thanks to the Cummins Turbo Technologies purchasing team, especially Alex Stelfox, for all the work carried out on the purchasing aspect of the project.

7. References

1. Burkinshaw, M. and Blacker, D. (2014). The high temperature tribological performance of turbocharger wastegate materials. *11th International Conference on Turbochargers and Turbocharging*. 1st Edition.
2. Tobar M, Amado J, Álvarez C, García A, Varela A, Yáñez A. Characteristics of Tribaloy T-800 and T-900 coatings on steel substrates by laser cladding. *Surface and Coatings Technology*. 2008; 202(11):2297-2301.
3. Vikström J. Galling resistance of hardfacing alloys replacing Stellite. *Wear*. 1994; 179(1-2):143-146.
4. Da Silva W, Souza R, Mello J, Goldenstein H. Room temperature mechanical properties and tribology of NICRALC and Stellite casting alloys. *Wear*. 2011; 271(9-10):1819-1827.
5. Ocken H. The galling wear resistance of new iron-base hardfacing alloys: a comparison with established cobalt- and nickel-base alloys. *Surface and Coatings Technology*. 1995; 76-77:456-461.
6. Datta P, Gray J. *Advances in surface engineering: Fundamentals of Coatings*. Cambridge: Royal Society of Chemistry; 1997.
7. Burakowski T, Wierzchoń T. *Surface engineering of metals*. Boca Raton, Fla.: CRC Press; 1999.
8. Cottis R, Shreir L, Lindsay R, Lyon S, Richardson J, Scantlebury J. *Shreir's corrosion*. Amsterdam [u.a.]: Elsevier; 2010.
9. Holmberg K, Matthews A. *Coatings tribology*. Amsterdam: Elsevier; 2009.
10. Vidakis N, Antoniadis A, Bilalis N. The VDI 3198 indentation test evaluation of a reliable qualitative control for layered compounds. *Journal of Materials Processing Technology*. 2003; 143-144:481-485.
11. Fuentes G, Almandoz E, Pierrugues R, Martínez R, Rodríguez R, Caro J. High temperature tribological characterisation of TiAlSiN coatings produced by cathodic arc evaporation. *Surface and Coatings Technology*. 2010; 205(5):1368-1373.
12. Johnson, K. (1987). *Contact mechanics*. Cambridge [u.a.]: Cambridge Univ. Press.
13. Li, C. and Bell, T. (2004). Corrosion properties of active screen plasma nitrided 316 austenitic stainless steel. *Corrosion Science*, 46(6), pp.1527-1547.
14. Fossati, A., Borgioli, F., Galvanetto, E. and Bacci, T. (2006). Corrosion resistance properties of glow-discharge nitrided AISI 316L austenitic stainless steel in NaCl solutions. *Corrosion Science*, 48(6), pp.1513-1527.
15. Kayali, Y., Büyüksağış, A., Güneş, I. and Yalçın, Y. (2013). Investigation of corrosion behaviors at different solutions of boronized AISI 316L stainless steel. *Protection of Metals and Physical Chemistry of Surfaces*, 49(3), pp.348-358.